Fatty Acid Transfer from *Yarrowia lipolytica* Sterol Carrier Protein 2 to Phospholipid Membranes

Lisandro J. Falomir Lockhart,[†‡] Noelia I. Burgardt,[‡§] Raúl G. Ferreyra,[‡§] Marcelo Ceolin,[‡¶] Mario R. Ermácora,[‡§] and Betina Córsico[†‡*]

[†]Instituto de Investigaciones Bioquímicas de La Plata (INIBIOLP), Facultad de Ciencias Médicas, Universidad Nacional de La Plata (UNLP), La Plata, Argentina; [‡]Consejo Nacional de Investigaciones Científicas y Técnicas (CONICET), Buenos Aires, Argentina; [§]Departamento de Ciencia y Tecnología, Universidad Nacional de Quilmes (UNQ), Bernal, Argentina; and [¶]Instituto de Físico-Química Teórica y Aplicada (INIFTA), Universidad Nacional de La Plata, La Plata, Argentina

ABSTRACT Sterol carrier protein 2 (SCP2) is an intracellular protein domain found in all forms of life. It was originally identified as a sterol transfer protein, but was recently shown to also bind phospholipids, fatty acids, and fatty-acyl-CoA with high affinity. Based on studies carried out in higher eukaryotes, it is believed that SCP2 targets its ligands to compartmentalized intracellular pools and participates in lipid traffic, signaling, and metabolism. However, the biological functions of SCP2 are incompletely characterized and may be different in microorganisms. Herein, we demonstrate the preferential localization of SCP2 of *Yarrowia lipolytica* (YLSCP2) in peroxisome-enriched fractions and examine the rate and mechanism of transfer of anthroyloxy fatty acid from YLSCP2 to a variety of phospholipid membranes using a fluorescence resonance energy transfer assay. The results show that fatty acids are transferred by a collision-mediated mechanism, and that negative charges on the membrane surface are important for establishing a "collisional complex". Phospholipids, which are major constituents of peroxisome and mitochondria, induce special effects on the rates of transfer. In conclusion, YLSCP2 may function as a fatty acid transporter with some degree of specificity, and probably diverts fatty acids to the peroxisomal metabolism.

INTRODUCTION

Several intracellular, soluble lipid-binding proteins (SLBPs) are deemed necessary to store and dissolve lipids, and transport them to and from the different intracellular compartments and membranes. Prominent examples are fatty acid-binding proteins (FABP) (1), acyl-CoA binding protein (ACBP) (2), sterol carrier protein 2 (SCP2) (3), oxysterol transfer protein (OSBP) (4), and a family of proteins called CRAL_TRIO, which includes the yeast phosphatidylinositol transfer protein Sec14 (5) and tocopherol transfer protein (6). In higher eukaryotes, several different SLBPs, and even several paralogs of the same SLBP, coexist within a cell. Furthermore, SLBPs differ in structure, phylogeny, intracellular localization, and binding properties.

In animals, SCP2 can be part of a variety of multidomain proteins localized in peroxisomes, mitochondria, and cytosol (7). On the other hand, fungal SCP2 generally is a stand-alone 14-kDa protein and seems to be strictly peroxisomal (8,9). Although it has been extensively studied in higher eukaryotes, the multiple roles of SCP2 in lipid metabolism have only recently begun to be appreciated. SCP-2 is involved in several steps of isoprenoid metabolism; increases the uptake, cycling, oxidation, and esterification of cholesterol; mediates the transfer of cholesterol and phospholipids between membranes; participates in phospholipid formation; has several roles in bile formation and secretion; is involved in the oxidation of branched side-chain lipids; and may participate in lipid signaling (reviewed in Schroeder et al. (3)). The functions of SCP2 in microorganisms are almost unknown, although it is believed to be important for peroxisomal oxidation of long-chain fatty acids (LCFAs).

The yeast *Yarrowia lipolytica* degrades hydrophobic substrates very efficiently by employing specific metabolic pathways (10). It grows profusely in a synthetic medium with sodium palmitate as the sole source of carbon and energy, and exhibits cytosolic LCFA-binding activity (11–13). Recently, our laboratory demonstrated that such activity is due to YLSCP2 (14) and gave an account of the general biophysical and binding properties of this protein. YLSCP2 is a single domain protein that is closely related to other SCP2 from fungi and multicellular eukaryotes, and binds cis-parinaric acid and palmitoyl-CoA with submicromolar affinity (14).

In this work we report the study of anthroyloxy fatty acid (AOFA) transfer from YLSCP2 to phospholipid membranes. The binding and relative partition coefficient of 16-(9-anthroyloxy) palmitic acid (16AP) between YLSCP2 and vesicles were determined, and the rates of transfer were analyzed as a function of vesicle concentration and composition, ionic strength, and temperature. It was found that transfer occurs by a collisional mechanism, and that changes in the surface charge and specificity of the acceptor vesicles can influence ligand transfer rates. Our results suggest that YLSCP2 may interact with membranes and transfer fatty acids to them in vivo. This issue is discussed in the context of the possible role of YLSCP2 in the peroxisomal metabolism of a lipid-degrading specialist such as *Y. lipolytica*.

Submitted August 23, 2008, and accepted for publication March 3, 2009.

*Correspondence: bcorsico@atlas.med.unlp.edu.ar

Editor: Marcia Newcomer.

0006-3495/09/07/0248/9 $2.00

doi: 10.1016/j.bpj.2009.03.063

MATERIALS AND METHODS

General details

AOFAs were purchased from Molecular Probes (Eugene, OR). Egg phosphatidylcholine (EPC), *N*-(7-nitro-2,1,3-benzoxadiazol-4-yl) phosphatidylcholine (NBD-PC), egg phosphatidylethanolamine (EPE), brain phosphatidylserine (PS), and bovine heart cardiolipin (CL) were obtained from Avanti Polar Lipids (Alabaster, AL). Isopropyl-β-D-thiogalactoside (IPTG) was obtained from Fisher (Fairlawn, NJ). Glass beads (0.4–0.6 mm diameter, acid-washed), 3,3′,5,5′ tetramethylbenzidine (TMB) liquid substrate system, and soy phosphatidylinositol (PI) were obtained from Sigma-Aldrich (St. Louis, MI). Polyclonal goat anti-rabbit immunoglobulin conjugated to HRP was obtained from DakoCytomation (Copenhagen, Denmark). All other chemicals were reagent grade or better. YLSCP2 concentration was determined by UV absorption using the published extinction coefficient (6986 M^{-1} cm^{-1}) (14). Protein concentration on yeast cell extracts was determined by a modification of the Lowry assay (15). The antiserum against YLSCP2 was generated in white rabbits by injections of pure recombinant YLSCP2 (0.2 mg emulsified in complete Freund's adjuvant) and used without purification (14). Nonlinear least-square fits were done with SigmaPlot (SPSS Science) (Chicago, IL) or with the Solver add-in in Excel (Microsoft).

Yeast strains and culture media

Saccharomyces cerevisiae MMY2: MAT α-*ura3* and *Y. lipolytica* CX 121 1B: *ade2* were generously provided by Professor J. R. Mattoon (University of Colorado, Colorado Springs, CO). Yeasts were grown aerobically at 28°C in YPD (1% yeast extract, 1% peptone, 1% glucose) or in YNB (0.67% yeast nitrogen base without amino acids) supplemented with 0.25% sodium palmitate (YNBP) or 1% glucose (YNBD). YPD was supplemented with 80 mg/L adenine hemisulfate or 50 mg/L uracil, as required.

Isolation of peroxisome-enriched fractions

Cells were grown for 48 h in YNBD medium, followed by growth for 24 h in fresh YNBP or YNBD media. They were then collected by centrifugation (3000 × *g*, 5 min), washed once with water, and resuspended in ice-cold, 0.6 M sorbitol, 20 mM Hepes, pH 7.4, 1 mM PMSF (0.5 g cells/mL). Two volumes of glass beads (0.4–0.6 mm diameter; Sigma-Aldrich, St. Louis, MI) were added to the cold suspension and the cells were broken by vigorous vortexing (three cycles of 30 s vortex and 30 s ice chilling). After the beads were removed, the resulting extracts were subjected to differential centrifugation at 4°C (first for 10 min at 700 × *g* to remove unbroken cells, nuclei, and debris, and then for 20 min at 20,000 × *g* to isolate a pellet (mostly peroxisomes and mitochondria) and a soluble (mostly cytosol) fraction). The pellet was resuspended in five volumes of PBS (150 mM NaCl, 150 mM sodium phosphate, pH 7.4).

Competence enzyme-linked immunosorbent assay

In succession, plate wells were coated for 2 h at room temperature with 2 ng/μL YLSCP2 in PBS (50 μL per well), washed with PBST buffer (PBS containing 0.5 M NaCl and 0.2% v/v Triton X-100), and blocked with BSA buffer (1% w/v bovine albumin in PBST). Then dilutions of each yeast extract fraction and a fixed volume of antiserum against YLSCP2, preincubated for 1 min in BSA buffer, were added to the wells (50 μL final volume per well) and incubated for 2 h at room temperature. After washing with PBST, 50 μL per well of HRP-linked anti-rabbit IgG antibody in BSA buffer was added, and the plates were incubated 2 h at room temperature. After a final wash with PBST, 50 μL per well of TMB liquid substrate system was added. Quantification of SCP2 in the samples was done by measuring absorbance at 450 nm using standard curves obtained with pure YLSCP2 processed in parallel. The specificity of the antiserum for YLSCP2 was confirmed by the absence of cross-reactivity in Western blots of *Y. lipolytica* and *S. cerevisiae* homogenates (not shown). Also, *S. cerevisiae* homogenates (a yeast that lacks a SCP2 gene) were used as control for nonspecific binding in the enzyme-linked immunosorbent assay (ELISA) assay, and the obtained values were subtracted from the *Y. lipolytica* samples.

Protein expression and purification

Recombinant YLSCP2 was expressed in *Escherichia coli* BL21 DE3 cells harboring pYLSCP2 (14). Protein expression was induced with 1 mM IPTG. YLSCP2 purification was performed as described previously (14). The procedure yields protein with the published sequence (http://www.ebi.ac.uk/embl/, accession AJ431362.2) and no additional residues. Briefly, after a 3-h induction, the cells were harvested by centrifugation, suspended in 10 mL of lysis buffer (50 mM Tris-HCl, 100 mM NaCl, 1.0 mM EDTA, pH 8.0), and disrupted by pressure (1000 psi; French Pressure Cell Press; Thermo IEC, Needham Heights, MA). Inclusion bodies isolated by centrifugation (15,000 × *g*, 10 min at 4°C) were first washed (14) and then solubilized in 25 mM sodium acetate, pH 5.5, 8 M urea, 10 mM glycine. The solution was clarified by centrifugation at 15,000 × *g* for 15 min at 4°C, and loaded into an SP Sepharose Fast-Flow (Pharmacia Biotech, Uppsala, Sweden) column (1.5 × 3.0 cm) equilibrated with solubilization buffer. Protein was eluted with a 200-mL linear gradient from 0 to 500 mM NaCl in solubilization buffer. Fractions containing pure YLSCP2 were pooled and subjected to refolding by dialysis (16 h, 5°C) against 1000 volumes of buffer A (50 mM sodium phosphate, pH 7.0). Finally, particulate matter was removed by centrifugation (16,000 × *g*, 30 min at 4°C).

Binding properties of recombinant YLSCP2

Fatty acid binding to YLSCP2 was assessed using a fluorescent titration assay (16). Briefly, 0.5 μM AOFA was incubated at 25°C for 5 min in buffer B (40 mM Tris 150 mM NaCl, pH 7.4) with increasing concentrations of YLSCP2. Then the fluorescence emission at 450 nm after excitation at 383 nm was recorded. The binding constant (K_D) was calculated assuming a single binding site (17) and fitting the equation

$$PL = 0.5\left[(P_T + L_T + K_D) - \sqrt{(P_T + L_T + K_D)^2 - 4P_TL_T}\right] \quad (1)$$

to the data, where PL, P_T, L_T, and K_D are the molar concentrations of the complex, total protein, total ligand, and dissociation constant, respectively. The equilibrium fluorescence signal was assumed to be

$$y = Y_P(P_T - PL) + Y_{PL}PL + Y_L(L_T - PL), \quad (2)$$

where Y_P, Y_{PL}, and Y_L are the fluorescence of the free protein, complex, and ligand, respectively. The binding constant was used to establish transfer conditions to ensure that most of the AOFA (at least 96%) was bound to YLSCP2 at time = 0.

Ligand partition between the protein and small unilamellar vesicles (SUVs) was determined by measuring AOFA fluorescence at different protein/SUV ratios obtained by adding SUV to a solution containing 2.5 μM protein and 0.25 μM AOFA in buffer B at 25°C (18,19). The relative partition coefficient (K_P) was defined as

$$K_P = \frac{AOFA_{SUV}\ YLSCP2}{AOFA_{YLSCP2}\ SUV}, \quad (3)$$

where $AOFA_{SUV}$ and $AOFA_{YLSCP2}$ are the concentrations of AOFA bound to membrane and YLSCP2, respectively, and YLSCP2 and SUV are the concentrations of protein and vesicles, respectively. The decrease in AOFA fluorescence as a function of *SUV* is related to K_p by

$$\frac{1}{\Delta F} = \frac{1}{\Delta F_{max}}\left[\frac{YLSCP2}{K_P\ SUV} + 1\right], \quad (4)$$

where ΔF is the difference between the fluorescence in the absence of vesicles and the fluorescence at a given YLSCP2/SUV ratio, and ΔF_{max} is the maximum difference in AOFA fluorescence with an excess of vesicles (20). A plot of $1/\Delta F$ versus $(1/\Delta F_{max})$(YLSCP2/SUV) has a slope of $1/K_P$. The partition coefficient was used to establish AOFA transfer assay conditions that ensure essentially unidirectional transfer, as detailed below.

Vesicle preparation

SUVs were prepared by sonication and ultracentrifugation as described previously (21,22). The standard vesicles contained EPC (EPC-SUV). To increase the negative charge density of the acceptor vesicles, either PE, PS, PI, or CL replaced EPC. Vesicles were prepared in buffer B, except for CL-containing SUVs, which were prepared in buffer B containing 1 mM EDTA. For AOFA transfer, 10 mol % of NBD-PC was incorporated into the mixture of phospholipids to serve as the fluorescent quencher of the antroyloxy derivative.

Transfer of AOFA from YLSCP2 to SUV

A fluorescence resonance energy transfer assay was used to monitor the transfer of AOFA from YLSCP2 to acceptor model membranes as described in detail elsewhere (23–25). Briefly, YLSCP2-bound AOFA was mixed at 25°C with SUVs using a Stopped-Flow RX-2000 (Applied Photophysics Ltd., UK) and the ensuing changes in fluorescence were monitored with an SLM-8000C spectrofluorometer (SLM Aminco Instruments Incorporated (Rochester, NY)). NBD is an energy-transfer acceptor for the anthroyloxy group, and therefore the fluorescence of AOFA is quenched when the ligand is incorporated into NBD-PC containing SUVs. Upon mixing, the kinetics of the transfer of AOFA from YLSCP2 to membranes was directly monitored by the decrease in AOFA fluorescence. The inal transfer assay conditions were 2.5 μM YLSCP2, 0.25 μM AOFA, and a range of 75–600 μM SUV. To ensure that photobleaching was negligible, appropriate controls were performed before each experiment. To analyze the transfer rate dependency with SUV superficial charge, SUVs with 25% negatively charged phospholipids were assayed. To analyze the effect of ionic strength, NaCl was varied from 0 to 2 M. The data were well described by a single-term exponential function. For each condition within a single experiment, at least five replicates were measured. The mean ± SE values for three or more separate experiments are reported.

Thermodynamic parameters of AOFA transfer

AOFA transfer from YLSCP2 to EPC-SUV was analyzed as a function of temperature. The activation energy (E_A) was calculated from the slope of the Arrhenius plot, and Eyring's rate theory was used to determine the thermodynamic parameters for the transfer process, as described previously (26). The enthalpy of transfer ($\Delta H^{\ddagger}$) was determined as $\Delta H^{\ddagger} = E_A - RT$, and the entropy was estimated as $\Delta S^{\ddagger} = R\ln(N\,h\,b\,e^{(\Delta H^{\ddagger}/RT)}R^{-1}\,T^{-1})$, where R, N, and h are the gas, Avogadro, and Planck constants, respectively, and b is the AOFA transfer rate from YLSCP2 to membranes at 25°C.

Circular dichroism spectroscopy

Circular dichroism (CD) measurements were carried out at 20°C on a Jasco 810 spectropolarimeter (Jasco, Japan). The scan speed was set to 50 nm/min, with a response time of 1 s, 0.2 nm pitch, and 1 nm bandwidth. Measurements were done with 0.1-cm optical-path quartz cells. The samples contained protein (5.6 μM) with or without SUVs (100% EPC) in 50 mM sodium phosphate pH 7.0. The relationship between YLSCP2 and SUV concentrations was 1:100. Five spectra were averaged for each sample.

RESULTS

YLSCP2 peroxisomal content

In a previous work, we demonstrated that the expression of YLSCP2 is inducible by fatty acids and accompanies the expansion of the peroxisomal compartment (11). In the study presented here, to estimate the intracellular concentration of induced YLSCP2, we developed an ELISA and applied it to analyze the cytoplasmic and peroxisome-enriched fractions of the yeast. After induction by palmitate, YLSCP2 accounted for 0.30 ± 0.05% (mean ± SE; $n = 5$) of the protein content of the organelle fraction, whereas in cells grown in glucose this content was 0.07 ± 0.04% (mean ± SE; $n = 4$). On the other hand, the YLSCP2 content of the cytoplasmic fractions was 0.21 ± 0.09 and 0.10 ± 0.03% (mean ± SE; $n = 5$) of total cytoplasmic protein for induced and noninduced cells, respectively. However, based on the proportion of catalase activity found in the cytoplasm (not shown), significant YLSCP2 leakage from the peroxisomal fraction during fractionation cannot be ruled out.

The ELISA results indicate that YLSCP2 is preferentially induced compared with total peroxisomal proteins (an ~fourfold induction). In absolute values, considering that the peroxisomal compartment as a whole is considerably expanded by fatty acid induction, the increase in YLSCP2 is much larger. Also, assuming a value of 15% total protein content for the peroxisomes, the concentration of YLSCP2 in the induced peroxisome can be roughly estimated as 30 μM. Previous estimates of the peroxisomal content of SCP2 for the closely related yeast *Candida tropicalis* growing on oleate yielded higher values (1.3% of the total peroxisomal protein) (12). Moreover, it was found that *C. tropicalis* SCP2 was strictly peroxisomal (12). The reasons for the differences are unknown. However, this study and the previous ones show that the peroxisomes of both species attain high SCP2 concentrations upon fatty acid induction.

Binding of fatty acid analogs to YLSCP2 and SUV

Preliminary experiments showed that YLSCP2 binds with submicromolar affinity to a variety of LCFA analogs (not shown). Among these, 16AP produced the largest increase in fluorescence emission upon binding and therefore was chosen for use in the transfer assays. The fit of Eq. 1 to the data for 16AP indicated one site per YLSCP2 molecule with a K_D of 60 ± 11 nM (mean ± SE, $n = 9$; Fig. 1).

The apparent partition coefficient that describes the relative distribution of 16AP between YLSCP2 and EPC-SUV was determined by adding EPC-SUV containing the energy transfer quencher NBD-PC to a solution of preformed 16AP-YLSCP2 complex. Analysis of the isotherms yielded a K_P of 2.6 ± 0.5 (Prot/SUV) (mean ± SE, $n = 7$; Fig. 2), which indicates the preferential partition of 16AP into phospholipid vesicles.

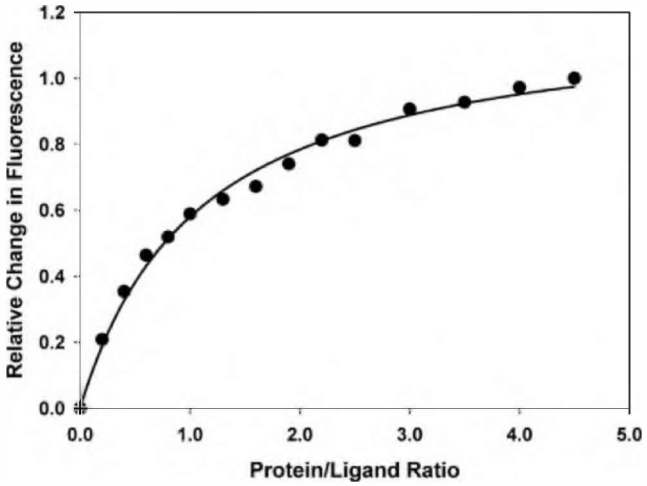

FIGURE 1 Binding isotherm of the YLSCP2-16AP complex. 16AP (0.5 μM) in buffer B was titrated at 25°C with increasing amounts of YLSCP2 from a concentrated stock solution in the same buffer. The fluorescence emission at 450 nm from a representative experiment is shown. One binding site per protein molecule was assumed. Equations 1 and 2 were fit to the data. The estimated K_D from nine independent experiments was 60 ± 11 nM (mean ± SE).

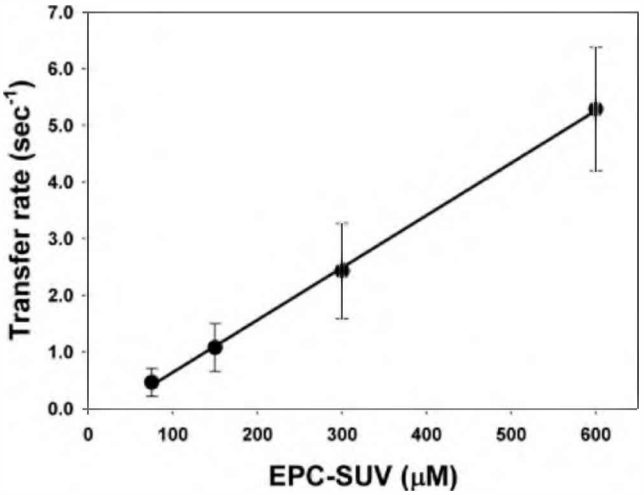

FIGURE 3 Dependence of the transfer rate of 16AP from YLSCP2 to membranes on SUV concentration. Transfer of 16AP from a preformed complex prepared by incubating 0.25 μM 16AP with 2.5 μM YLSCP2 to NBD-containing zwitterionic EPC-SUV was measured as a function of SUV concentration. The donor complex and receptor membrane were both in buffer B at 25°C. Transfer rates (mean ± SE; $r^2 = 0.9994$) from five or more experiments are shown.

Effect of vesicle concentration

In a collisional transfer, the limiting step is the effective protein-membrane interaction, and the rate increases as the acceptor membrane concentration increases. In a diffusional mechanism in which the rate-limiting step is the dissociation of the protein-ligand complex, no change in rate is observed (16,23–27). The values of K_D and K_P were used to set the conditions for the transfer assay. The proportion of protein and ligand was such that <4% of AOFA remained free in the preincunbation solution. On the other hand, the K_P value was used to calculate the final concentrations of protein and SUVs for which unidirectional transfer prevailed. Fig. 3 shows that when constant concentrations of the YLSCP2-16AP donor complexes were mixed with increasing concentrations of EPC-SUV, the 16AP transfer rate from YLSCP2 to EPC-SUV increased proportionally to vesicle concentration over an SUV:YLSCP2 ratio of 30:1 to 240:1. In these conditions, the increase in transfer rate ranged from 0.47 ± 0.21 s^{-1} to 5.29 ± 1.09 s^{-1} (corresponding to 75–600 μM SUV, respectively). These results strongly suggest that the fatty acid transfer from YLSCP2 occurs via a protein-membrane interaction rather than by simple aqueous diffusion of the free ligand.

Effects of vesicle composition

In a collisional mechanism, membrane properties, particularly the surface net charge, should influence the rate of transfer. In the case of a diffusional mechanism, the properties of the acceptor membrane would be much less important, since the rate-determining step is likely to be the ligand dissociation from the protein into the aqueous phase (24,27). Fig. 4 *A* shows that the 16AP transfer rate from YLSCP2 increases nearly fourfold when 25% PS is incorporated into EPC/NBD-PC acceptor membranes (from 1.14 ± 0.45 to 4.46 ± 1.93 s^{-1}). Incorporation of 25% CL in the acceptor vesicles resulted in a dramatic 47-fold rate increase, which cannot be explained exclusively by the twofold increase in the surface net negative charge compared to

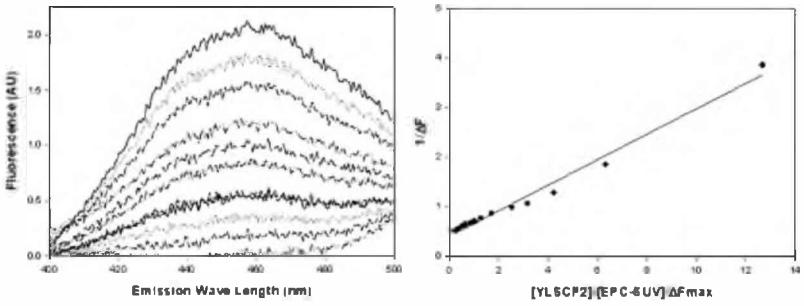

FIGURE 2 Equilibrium partition of 16AP between membranes and YLSCP2. The K_p (protein-bound 16AP/membrane-bound 16AP) was determined by titrating at 25°C a solution of 0.25 μM 16AP, 2.5 μM YLSCP2 with NBD-containing zwitterionic EPC-SUV, both in buffer B. The ensuing change in fluorescence emission at 450 nm was recorded, and Eq. 4 was fit to the data. A representative experiment is shown. Seven independent experiments were performed to calculate a K_p of 2.6 ± 0.5 (mean ± SE).

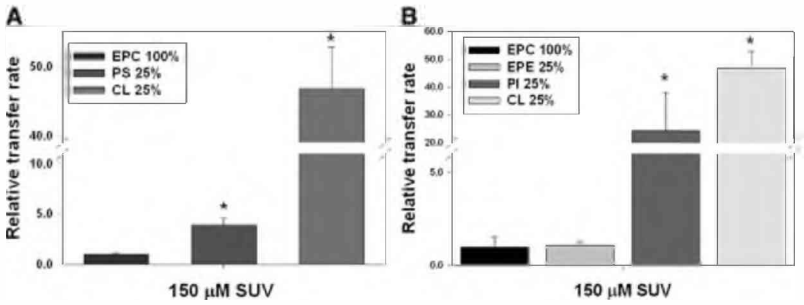

FIGURE 4 Effect of SUV composition on the transfer rate of 16AP from YLSCP2 to membranes. Transfer of 16AP from a preformed complex, prepared by incubating 0.25 μM 16AP with 2.5 μM YLSCP2, to 150 μM NBD-containing SUV of different superficial net charge. In panel *A*, to increase negative charges, 25 mol % of PS or CL was replaced in the composition of EPC-SUV. Panel *B* shows the effect of 25 mol % replacement with phospholipids enriched in the peroxisomal compartment (EPE, PI, and CL). Results are expressed relative to the transfer to EPC-SUV (1.14 s^{-1} $\pm$ 0.21; * $p < 0.01$).

PS. Therefore, we analyzed the effect of other lipids that are characteristic of peroxisomal membranes, such as PE and PI. The incorporation of 25% EPE into acceptor membranes did not result in significant modifications of the transfer rate compared to zwitterionic vesicles (1.07 $\pm$ 0.09 s^{-1}; Fig. 4 *B*). On the other hand, SUVs containing PI showed an ~25-fold increase (27.70 $\pm$ 7.8), which, as in the case of CL, is probably pointing to a specific effect of PI. Taken together, these results also support a collisional mechanism of FA transfer for YLSCP2.

Effect of ionic strength

The rate of transfer of a hydrophobic molecule from a binding protein by diffusion in an aqueous phase to an acceptor membrane should be modulated by factors that alter its aqueous solubility, whereas collisional transfer is likely to be unaffected (28,29). Thus, the transfer of 16AP from YLSCP2 to membranes was examined as a function of increasing concentrations of NaCl. The 16AP transfer rate from YLSCP2 to SUV (150 μM) does not significantly change when the salt concentration is varied from 0 to 1 M, and only a small decrease is observed above 1 M NaCl (Fig. 5).

Effect of temperature

The effect of temperature (5–45°C) on 16AP transfer from YLSCP2 to EPC-SUV was assessed to calculate the thermodynamic parameters of the process. The results are shown as an Arrhenius plot in Fig. 6. The transfer rates increased with temperature according to an endothermic process. The Arrhenius plot was linear, indicating no significant deviation from the theory. The thermodynamic parameters derived using Eyring's rate theory (26) are presented in Table 1. The results show a much larger contribution of the enthalpic term compared with that of the entropic term and a $\Delta G^{\ddagger}$ of 18.1 $\pm$ 0.1 kcal/mol. This result may reflect a central role of noncovalent interactions between the protein and the membrane during collisional transfer of 16AP, whereas changes in bulk water order would be less important.

YLSCP2 interaction with SUV

The far-UV CD spectra of YLSCP2 alone or in the presence of an excess of SUV is shown in Fig. 7. The spectral changes reveal an increase in the α-helix content of the protein in the presence of vesicles. Since incubation with fatty acids, phospholipids, or cholesterol fails to induce significant changes in the far-UV spectrum of YLSCP2 (Burgardt et al., unpublished results), the result is consistent with a direct interaction between the protein and the membranes.

DISCUSSION

SLBPs are thought to participate in the intracellular transport and storage of hydrophobic compounds, and to mediate lipid exchange between membranes (1–5). However, there is such a variety of SLBPs, and they are so diversely and redundantly distributed in organisms, tissues, cells, and organelles, that their effects and the mechanism by which they function must be evaluated on a case-by-case basis.

The only known SLBPs that are able to bind fatty acids in yeasts are SCP2 and ACBP; however, ACBP does not bind unesterified LCFA (2), which leaves SCP2 as the only candidate for LCFA transport in these microorganisms. Moreover,

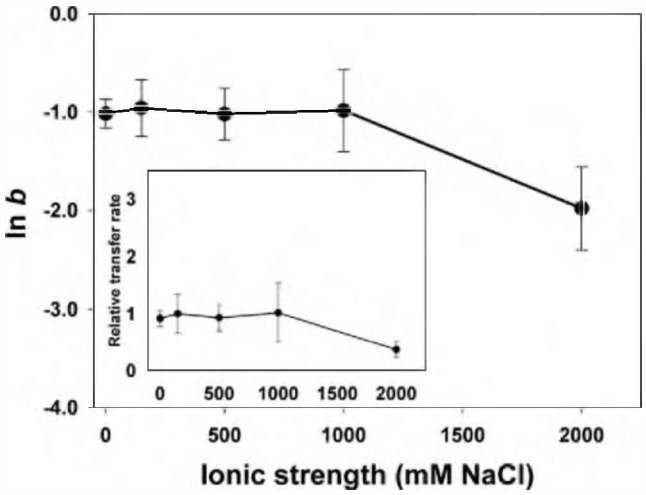

FIGURE 5 Effect of ionic strength on 16AP transfer from YLSCP2 to membranes. Transfer of 16AP from a preformed complex, prepared by incubating 0.25 μM 16AP with 2.5 μM YLSCP2, to NBD-containing zwitterionic EPC-SUV was measured as a function of NaCl concentration. The NaCl concentrations of donor and acceptor were adjusted before mixing. For clarity, ln (*b*) is shown as a function of NaCl concentration, where *b* is the transfer rate of 16AP. Also, mean $\pm$ SE transfer rates from five or more experiments are shown in the inset.

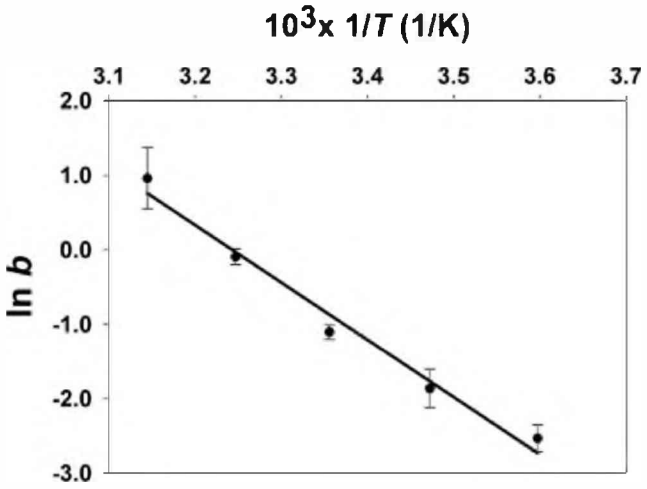

FIGURE 6 Effect of temperature on 16AP transfer from YLSACP2 to membranes. Transfer of 16AP from a preformed complex, prepared by incubating 0.25 μM 16AP with 2.5 μM YLSCP2, to 150 μM NBD-containing zwitterionic EPC-SUV was monitored at 10°C intervals from 5 to 45°C. The data were analyzed as described in Materials and Methods. Transfer rates (mean ± SE) from three separate experiments are shown in the Arrhenius plot, where b is the transfer rate ($r^2 = 0.98$).

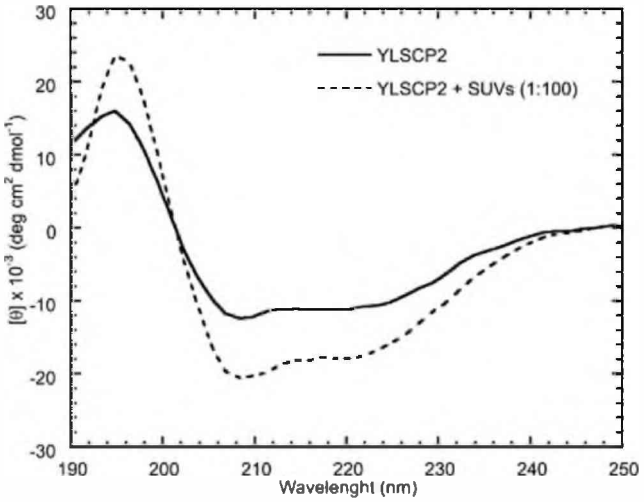

FIGURE 7 Far-UV CD changes induced by SUV. YLSCP2 was incubated in 50 mM sodium phosphate pH 7.0 (*full line*) and in the same buffer with the addition of EPC-SUV (*dashed line*).

yeast SCP2 is believed to be located in peroxisomes (30), raising the question of whether this organelle is the only yeast compartment with the potential to attain concentrations of protein-solubilized LCFA and CoA esters of LCFA larger than the CMC. In an attempt to shed some light on the relationship between LCFA traffic and SLBP in yeast, we set out to study SCP2 in *Y. lipolytica*. This microorganism is a particularly good experimental system because of its well-known voracity for fatty acids and ability to feed on these compounds as the only source of carbon and energy.

Our study confirmed that YLSCP2 is strongly induced by palmitic acid and preferentially located in the peroxisomal fraction of the yeast. The magnitude of the induction exceeds by severalfold the expansion of the peroxisomal compartment elicited by the inductor. This clearly indicates that the protein has a role beyond accompanying peroxisomal proliferation, and points to an important participation in the metabolism of lipids. A large body of in vivo and in vitro experimental evidence supports a role of mammalian SCP2 in lipid uptake and diffusion (3,31,32). In mammals, the SCP2 domain is located in peroxisomes, mitochondria, and the cytosol, which introduces further complexity into the analysis of its function (7). Unfortunately, the results obtained with *Y. lipolytica* do not eliminate the possibility of a cytosolic localization for SCP2; however, the measured high concentration of YLSCP2 in the peroxisome, and the high affinity of YLSCP2 for LCFA and their CoA esters lend probability to the hypothesis that one of the functions of yeast SCP2 may be to facilitate lipid uptake by the peroxisome.

TABLE 1 Activation parameters of AOFA transfer from YLASCP2 to phospholipid membranes

E_A	15.5 ± 1.9 kcal/mol
$\Delta H^{\ddagger}$	14.6 ± 1.9 kcal/mol
$T\Delta S^{\ddagger}$	3.5 ± 1.9 kcal/mol
$\Delta G^{\ddagger}$	18.1 ± 0.1 kcal/mol

E_A was calculated from the Arrhenius plots in the range of 5–45°C (Fig. 6). $\Delta H^{\ddagger}$, $\Delta G^{\ddagger}$, and $T\Delta S^{\ddagger}$ were calculated at 25°C as described in Materials and Methods. Units are kcal/mol, and the mean ± SE values of three separate experiments are listed.

Given the above hypothesis, we sought to analyze the ability of YLSCP2 to act as a fatty acid transfer protein. We conducted protein-to-membrane transfer assays employing the anthroyloxy-labeled fatty acid 16AP, and therefore first assessed the binding and partitioning characteristics of this protein-ligand system. In previous works, we determined the affinity of AOFA for several SLBPs (16,23,33). In this work, employing the same fluorescent titration assay, we found that the K_D value for the interaction of 16AP and YLSCP2 (60 ± 11 nM) is comparable to that of anthroyloxy oleic acid for intestinal and liver FABP (160 ± 40 nM and 20 ± 10 nM, respectively), two members of the FABP family that are known to be heavily expressed in mammal enterocytes. The affinity of YLSCP2 for 16AP is also comparable to its affinity for *cis*-parinaric acid (81 ± 40 nM) and palmitoyl CoA (73 ± 33 nM) (14). Thus, 16AP is a suitable probe for protein-membrane transfer experiments involving YLSCP2. The in vitro partition of 16AP between YLSCP2 and membranes was found to favor the SUV ($K_P = 2.6$). We previously found that the relative affinity of AOFAs for protein compared with membrane varies widely in the FABP family: from 0.09, as observed for LFABP, to 6.74 for IFABP (25). The fact that K_D and K_P values for YLSCP2 fall between those of IFABP and LFABP or LbFABP (33) confirms the relationship between protein affinity (K_D) and EPC-SUV relative affinity (K_P).

The nature of the interaction between SLBPs and membranes has been extensively examined with the use of artificial membranes and fluorescence resonance energy transfer, which can directly monitor the kinetics of fatty acid transfer (1). In this work, we applied that biophysical approach to the functional study of a member of the SCP2 family of proteins. The results provide the first evidence (to our knowledge) of the fatty acid transfer activity of YLSCP2 to phospholipid membranes.

Previous studies demonstrated that different SLBPs use two distinct transfer mechanisms according to whether they collect or deliver their ligands by contact with a membrane (collisional transfer), or whether the ligand must enter the solvent phase during the exchange (diffusional transfer) (1,16,23–27,34). The former are considered to be involved in the intracellular trafficking of lipids between cell membranes, whereas the latter do not interact directly with membranes and are considered lipid-storage system. Also, it is hypothesized that fatty acid transfer from "collisional" SLBP involves targeted interactions of the protein with specific membrane domains. Most of the FABPs studied so far (i.e., FABPs of intestine, adipocyte, heart, and brain) show a collisional mechanism of transfer. In contrast, transfer from LFABP and cellular retinol binding protein II occurs by a diffusional mechanism (1). In the case of mammalian SCP2, several lines of evidence indicate that a direct interaction between the protein and membranes occurs during transfer (35,36).

The evidence presented herein indicates that AOFAs are transferred from YLSCP2 to vesicles during collisional interactions (Fig. 8 *A*). First, the ligand transfer rate increases in direct proportion to the concentration of acceptor vesicles, as expected for concentration-dependent collisional events. Second, the transfer rate is highly sensitive to the charge of the acceptor vesicles, with an increase for negatively charged membranes. By varying the lipid composition of the target membranes, we identified CL- and PI-containing vesicles as very efficient acceptors. The modulation of ligand transfer rate by acceptor membrane properties is a hallmark of collisional transfer, because a diffusion-mediated mechanism would not be as responsive. This result is particularly important because it was recently reported that CL and PI are normal components of the peroxisomes in the yeasts *Pichia pastori* and *S. cerevisiae* (37,38), which may reveal a specific mechanism of LCFA targeting. Although, in principle, changes in lipid composition could also affect other membrane properties, such as size, curvature, differential composition domain formation, and fluidity, most of these possibilities were ruled out in a previous work in which we demonstrated that there was no change in vesicle size and curvature in a broad range of lipid compositions as long as the number of acyl chains was maintained (27). Moreover, the formation of membrane microdomains with distinct properties is not to be expected under the conditions used in these experiments (39). Finally, alteration of the ionic strength has little effect on the AOFA transfer rate, further supporting a collisional model. If the transfer were diffusional, the reduction of free ligand concentration induced by the decrease in water activity would slow down the rate, as observed for LFABP (16,34), a well-established model for the diffusional mechanism. The lack of effect of increasing the ionic strength on the rate of transfer to zwitterionic vesicles can be explained by opposite and compensated electrostatic and hydrophobic interactions involving the formation of the protein-membrane complex, as observed for IFABP, a well-established collisional FABP (16,34).

The thermal dependence of the transfer rate revealed additional aspects of the process. The calculated $\Delta G^{\ddagger}$ arises mostly from enthalpy changes, with a relatively small entropy contribution. A similar relationship between $\Delta H^{\ddagger}$

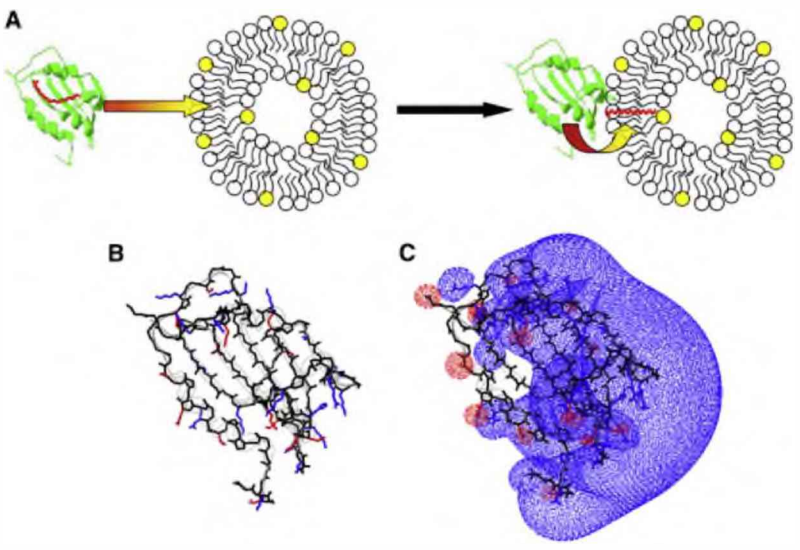

FIGURE 8 Fatty acid transfer mechanism. Panel *A* depicts the proposed collisional mechanism of ligand transfer from YLSCP2 to membranes. The interacting region of the protein was assumed to be the positively charged side shown in panels *B* and *C*. The model of YLSCP2 was obtained by homology modeling using an algorithm implemented in the program 3D-JIGSAW2.0 (41), and rabbit SCP2 (PDB ID: 1c44) as a template (Burgardt et al., unpublished results). A mammalian SCP2 was chosen as the template because of its higher sequence homology to YLSCP2 (30% identity) than insect or bacterial templates (20–25% identity). The fatty acid orientation in the binding site is one of the possible orientations seen in the crystal structures of insect SCP2 (PDB ID: 1PZ4 and 2QZT) The SPDViewer program was used to represent the YLSCP2 model, the unequal distribution of charged residues, and the prominent surface electrostatic potential of the protein. Negatively charged residues and negative electrostatic potential are highlighted in red, and positively charged residues and positive electrostatic potential are shown in blue.

and $T\Delta S^{\ddagger}$ was reported for collisional FABP (34). In contrast, the free energy of AOFA transfer from a diffusional FABP is composed of equally important enthalpy and entropy components (26). Although $\Delta G^{\ddagger}$ for AOFA transfer from YLSCP2 and a collisional FABP is somewhat smaller than that for transfer from a diffusional FABP, the associated change in enthalpy is greater. Thus, in the formation of the activated complex YLSCP2-AOFA-membrane, the noncovalent interactions are crucial. These interactions may involve not only AOFA within the YLSCP2 binding site, but also the transient association of YLSCP2 with the acceptor membranes and the associated conformational changes of the protein.

To directly investigate the interaction between YLSCP2 and membranes, we analyzed the equilibrium CD spectra of YLSCP2 in the presence of membranes compared with the protein alone. Of interest, the interaction caused a conformational change in the protein. This finding is in agreement with previous reports regarding the interaction of human SCP2 with anionic SUV (35), and further supports our hypothesis of a collisional interaction in the transfer process.

The importance of electrostatic interactions between cationic residues on the protein surface and anionic membrane phospholipid headgroups, as well as a lesser contribution of hydrophobic interactions, has been demonstrated for FABPs that transfer ligand by a collisional mechanism (27). A positive surface electrostatic potential across the helix-turn-helix portal region of collisional FABP, together with the amphipathic character of their α-I helices, suggests the involvement of this region in the interaction with membranes (25,40). Further structure-function analysis using structural variants of FABP strongly supports the centrality of the α-helical region in determining the ligand transfer mechanism (16,23–25). For mammalian SCP2, it was reported that cholesterol transfer was the highest in membranes containing acidic phospholipids (35). Even though a crystal or NMR structure of YLSCP2 is not yet available, a structural homology model predicts a extended region of net positive surface charge formed by residues $Lys^{29,34,35,104,106,108,113,122}$ and Arg^{98} that may be involved in membrane interaction (Burgardt et al., unpublished results; Fig. 8, *B* and *C*). This region includes mostly residues from the C-terminus (on the *right side* of the cartoons in Fig. 8, *B* and *C*), but also part of helix 2 at the N-terminus (at the *top* of Fig. 8, *B* and *C*). The electrostatic pattern of YLSCP2 is present in mammalian SCP2, but is much less evident in bacterial and insect SCP2 (not shown). The differential electrostatic pattern between these SCP2s may reflect membrane interaction by different mechanisms or the lack thereof. Of interest, the N-terminal amphipathic helix of mammalian SCP2 (residues 1–32) was found to be essential for sterol transfer, and, although inactive by itself, it nevertheless enhanced the activity of the whole SCP2 in that regard (36). If the transfer in mammal and yeast is mediated by the same surface region, the above observation is congruent with the participation of $Lys^{29,34,35}$ in the positively-charged membrane-binding region proposed herein for YLSCP2. These structural predictions provide a promising starting point for future works aimed at characterizing the specific contributions of the above-mentioned residues in the transfer process by site-directed mutagenesis.

We conclude that YLSCP2 possesses all the attributes necessary to function as an important factor in the transport of LCFA in *Y. lipolytica*, and its behavior with membranes of different lipid composition could indicate some specificity that may be important for targeting fatty acids and their derivatives to peroxisomes.

The work was supported by the Agencia Nacional de Promoción Científica y Tecnológica, Argentina (BID 1728/OC-AR PICT 25892). M.C. is full professor at Universidad Nacional del Noroeste de Buenos Aires.

REFERENCES

1. Storch, J., and B. Corsico. 2008. The emerging functions and mechanisms of mammalian fatty acid-binding proteins. *Annu. Rev. Nutr.* 28:73–95.
2. Kragelund, B. B., J. Knudsen, and F. M. Poulsen. 1999. Acyl-coenzyme A binding protein (ACBP). *Biochim. Biophys. Acta.* 1441:150–161.
3. Schroeder, F., B. P. Atshaves, A. L. McIntosh, A. M. Gallegos, S. M. Storey, et al. 2007. Sterol carrier protein-2: new roles in regulating lipid rafts and signaling. *Biochim. Biophys. Acta.* 1771:700–718.
4. Beh, C. T., G. Alfaro, G. Duamel, D. P. Sullivan, M. C. Kersting, et al. 2009. Yeast oxysterol-binding proteins: sterol transporters or regulators of cell polarization? Genome-wide analysis of sterol-lipid storage and trafficking in *Saccharomyces cerevisiae*. *Mol. Cell. Biochem.* 7:401–414.
5. Schaaf, G., E. A. Ortlund, K. R. Tyeryar, C. J. Mousley, K. E. Ile, et al. 2008. Functional anatomy of phospholipid binding and regulation of phosphoinositide homeostasis by proteins of the sec14 superfamily. *Mol. Cell.* 29:191–206.
6. Morley, S., M. Cecchini, W. Zhang, A. Virgulti, N. Noy, et al. 2008. Mechanisms of ligand transfer by the hepatic tocopherol transfer protein. *J. Biol. Chem.* 283:17797–17804.
7. Martin, G. G., H. A. Hostetler, A. L. McIntosh, S. E. Tichy, B. J. Williams, et al. 2008. Structure and function of the sterol carrier protein-2 N-terminal presequence. *Biochemistry.* 47:5915–5934.
8. Edqvist, J., and K. Blomqvist. 2006. Fusion and fission, the evolution of sterol carrier protein-2. *J. Mol. Evol.* 62:292–306.
9. Tan, H., K. Okazaki, I. Kubota, T. Kamiryo, and H. Utiyama. 1990. A novel peroxisomal nonspecific lipid transfer protein from *Candida tropicalis*. Gene structure, purification and possible role in β oxidation. *Eur. J. Biochem.* 190:107–112.
10. Fickers, P., P. H. Benetti, Y. Wache, A. Marty, S. Mauersberger, et al. 2005. Hydrophobic substrate utilisation by the yeast *Yarrowia lipolytica*, and its potential applications. *FEMS Yeast Res.* 5:527–543.
11. Dell'Angelica, E. C., M. R. Ermácora, and J. A. Santomé. 1996. Purification and partial characterization of a fatty acid binding protein from the yeast *Yarrowia lipolytica*. *Biochem. Mol. Biol. Int.* 39:439–445.
12. Dell'Angelica, E. C., C. A. Stella, M. R. Ermácora, E. H. Ramos, and J. A. Santomé. 1992. Study on fatty acid binding by proteins in yeast. Dissimilar results in *Saccharomyces cerevisiae* and *Yarrowia lipolytica*. *Comp. Biochem. Physiol. B.* 102:261–265.
13. Dell'Angelica, E. C., C. A. Stella, M. R. Ermácora, J. A. Santomé, and E. H. Ramos. 1993. Inhibitory action of palmitic acid on the growth of *Saccharomyces cerevisiae*. *Folia Microbiol. (Praha).* 38:486–490.
14. Ferreyra, R. G., N. I. Burgardt, D. Milikowski, G. Melen, A. R. Kornblihtt, et al. 2006. A yeast sterol carrier protein with fatty-acid and fatty-acyl-CoA binding activity. *Arch. Biochem. Biophys.* 453:197–206.

15. Peterson, G. L. 1983. Determination of total protein. *Methods Enzymol.* 91:95–119.

16. Corsico, B., H. L. Liou, and J. Storch. 2004. The α-helical domain of liver fatty acid binding protein is responsible for the diffusion-mediated transfer of fatty acids to phospholipid membranes. *Biochemistry.* 43:3600–3607.

17. Miller, D. M., J. S. Olson, J. W. Pflugrath, and F. A. Quiocho. 1983. Rates of ligand binding to periplasmic proteins involved in bacterial transport and chemotaxis. *J. Biol. Chem.* 258:13665–13672.

18. Storch, J., C. Lechene, and A. M. Kleinfeld. 1990. Mechanism for binding of fatty acids to hepatocyte plasma membranes: different interpretation. *J. Biol. Chem.* 12:1447–1449.

19. Massey, J. B., D. H. Bick, and H. J. Pownall. 1997. Spontaneous transfer of monoacyl amphiphiles between lipid and protein surfaces. *Biophys. J.* 72:1732–1743.

20. Roseman, M. A., and T. E. Thompson. 1980. Mechanism of the spontaneous transfer of phospholipids between bilayers. *Biochemistry.* 19:439–444.

21. Huang, C., and T. E. Thompson. 1974. Preparation of homogeneous, single-walled phosphatidylcholine vesicles. *Methods Enzymol.* 32:485–489.

22. Storch, J., and P. G. Munder. 1986. Transfer of long-chain fluorescent free fatty acids between unilamellar vesicles. *Lipids.* 25:1717–1726.

23. Corsico, B., D. P. Cistola, C. Frieden, and J. Storch. 1998. The helical domain of intestinal fatty acid binding protein is critical for collisional transfer of fatty acids to phospholipid membranes. *Proc. Natl. Acad. Sci. USA.* 95:12174–12178.

24. Falomir-Lockhart, L. J., L. Laborde, P. C. Kahn, J. Storch, and B. Corsico. 2006. Protein-membrane interaction and fatty acid transfer from intestinal fatty acid-binding protein to membranes. Support for a multistep process. *J. Biol. Chem.* 281:13979–13989.

25. Franchini, G. R., J. Storch, and B. Corsico. 2008. The integrity of the α-helical domain of intestinal fatty acid binding protein is essential for the collision-mediated transfer of fatty acids to phospholipid membranes. *Biochim. Biophys. Acta.* 1781:192–199.

26. Kim, H. K., and J. Storch. 1992. Free fatty acid transfer from rat liver fatty acid-binding protein to phospholipid vesicles. Effect of ligand and solution properties. *J. Biol. Chem.* 267:77–82.

27. Corsico, B., G. R. Franchini, K. T. Hsu, and J. Storch. 2005. Fatty acid transfer from intestinal fatty acid binding protein to membranes: electrostatic and hydrophobic interactions. *J. Lipid Res.* 46:1765–1772.

28. Charlton, S. C., and L. C. Smith. 1982. Kinetics of transfer of pyrene and rac-1-oleyl-2-[4-(3-pyrenyl)butanoyl]glycerol between human plasma lipoproteins. *Biochemistry.* 21:4023–4030.

29. Constantinides, P. P., and J. M. Steim. 1985. Physical properties of fatty acyl-CoA. Critical micelle concentrations and micellar size and shape. *J. Biol. Chem.* 260:7573–7580.

30. Tan, H., M. Bun-Ya, A. Hirata, and T. Kamiryo. 1994. Predominant localization of non-specific lipid-transfer protein of the yeast *Candida tropicalis* in the matrix of peroxisomes. *Yeast.* 10:1065–1074.

31. McArthur, M. J., B. P. Atshaves, A. Frolov, W. D. Foxworth, A. B. Kier, et al. 1999. Cellular uptake and intracellular trafficking of long chain fatty acids. *J. Lipid Res.* 40:1371–1383.

32. Gallegos, A. M., B. P. Atshaves, S. M. Storey, O. Starodub, A. D. Petrescu, et al. 2001. Gene structure, intracellular localization, and functional roles of sterol carrier protein-2. *Prog. Lipid Res.* 40:498–563.

33. Di Pietro, S. M., B. Corsico, M. Perduca, H. L. Monaco, and J. A. Santome. 2003. Structural and biochemical characterization of toad liver fatty acid-binding protein. *Biochemistry.* 42:8192–8203.

34. Hsu, K. T., and J. Storch. 1996. Fatty acid transfer from liver and intestinal fatty acid-binding proteins to membranes occurs by different mechanisms. *J. Biol. Chem.* 271:13317–13323.

35. Huang, H., J. M. Ball, J. T. Billheimer, and F. Schroeder. 1999. The sterol carrier protein 2 amino terminus: a membrane interaction domain. *Biochemistry.* 38:13231–13243.

36. Huang, H., A. M. Gallegos, M. Zhou, J. M. Ball, and F. Schroeder. 2002. Role of the sterol carrier protein-2 N-terminal membrane binding domain in sterol transfer. *Biochemistry.* 41:12149–12162.

37. Wriessnegger, T., G. Gubitz, E. Leitner, E. Ingolic, J. Cregg, et al. 2007. Lipid composition of peroxisomes from the yeast *Pichia pastoris* grown on different carbon sources. *Biochim. Biophys. Acta.* 1771:455–461.

38. Zinser, E., C. D. Sperka-Gottlieb, E. V. Fasch, S. D. Kohlwein, F. Paltauf, et al. 1991. Phospholipid synthesis and lipid composition of subcellular membranes in the unicellular eukaryote *Saccharomyces cerevisiae*. *J. Bacteriol.* 173:2026–2034.

39. Shibata, A., K. Ikawa, T. Shimooka, and H. Terada. 1994. Significant stabilization of the phosphatidylcholine bilayer structure by incorporation of small amounts of cardiolipin. *Biochim. Biophys. Acta.* 1192:71–78.

40. LiCata, V. J., and D. A. Bernlohr. 1998. Surface properties of adipocyte lipid-binding protein: Response to lipid binding, and comparison with homologous proteins. *Proteins.* 33:577–589.

41. Bates, P. A., L. A. Kelley, R. M. MacCallum, and M. J. Sternberg. 2001. Enhancement of protein modeling by human intervention in applying the automatic programs 3D-JIGSAW and 3D-PSSM. *Proteins.* (Suppl 5):39–46.